Journal of Advanced Research in Applied Sciences and Engineering Technology

Journal homepage:

https://semarakilmujournal.com.my/index.php/araset
ISSN: 2462-1943

Effect of Stereolithography (SLA) Machine Printing Parameters on Mechanical Properties and Surface Characteristics of Polylactid Acid (PLA)

Aris Sandi[1,*], Juan Pratama[2], Sukmaji Indro Cahyono[3], Urip Agus Salim[4], Muslim Mahardika[4], Budi Arifvianto[4]

[1] Department of Plantation Industrial Machinery Engineering Technology, Politeknik LPP, Yogyakarta 55222, D.I. Yogyakarta, Indonesia
[2] Department of Mechanical Engineering, Faculty of Engineering, Darma Persada University, East Jakarta 13450, Jakarta, Indonesia
[3] Department of Mechanical Engineering, Sebelas Maret University, Surakarta 57126, Central Java, Indonesia
[4] Department of Mechanical and Industrial Engineering and Centre for Innovation of Medical Equipment and Devices (CIMEDs), Faculty of Engineering, Universitas Gadjah Mada, Sleman 55281, D.I. Yogyakarta, Indonesia

ARTICLE INFO

Article history:
Received 2 March 2026
Received in revised form 7 March 2026
Accepted 15 March 2026
Available online 7 April 2026

Keywords:

Stereolithography; Layer thickness; Normal exposure time; Mechanical strength; Surface characterization; Polylactic acid

ABSTRACT

The research aims to investigate the effects of printing parameters on the mechanical properties and surface characteristics of polylactic acid (PLA) material processed by stereolithography. PLA specimens were printed with variable parameters of layer thickness (0.025, 0.05, and 0.075 mm) and normal exposure time (5, 10, and 15 s), while the fixed parameters were a 90° build orientation (transversal, along the X-axis), washing time of 5 min, and curing time of 30 min. Mechanical and surface-characteristics tests were performed on printed specimens to determine the effects of SLA printing parameters on tensile strength, elastic modulus, and surface characteristics. The results showed that the tensile strength, elongation, and surface roughness of the SLA printed specimens were not sensitive to variations in LT and NET in this research except for dimensional accuracy. The combination of LT 0.05 mm and NET 10 seconds produced specimens with the highest mechanical strength, compared with the smaller LT 0.025 mm combined with NET 15 seconds. The similar phenomenon was also observed in the surface roughness test, where a random pattern was observed in the results across various measurement directions (horizontal, vertical, and diagonal). However, the lowest average roughness was obtained with the parameter LT set to 0.025 mm and a NET of 10 seconds. This differs from the pattern of data obtained in the dimensional accuracy test, where the lowest deviation is found in the parameter LT, 0.075 mm, with NET 10 seconds.

1. Introduction

Manufacturing technology is advancing rapidly worldwide. This is evident in the many new research results from researchers across various disciplines, such as additive manufacturing (AM). AM is the process of making physical objects from the results of geometric representations in computer-aided design (CAD) software, where the production process is carried out by adding

* *Corresponding author.*
E-mail address: aris@polteklpp.ac.id

https://doi.org/10.37934/araset.58.5.5874

material sequentially or layer by layer [1]. In everyday life, especially in the manufacturing industry, AM technology is commonly known as 3D printing (3DP).

3DP technology is a method of making mechanical products with several advantages, such as printing complex geometries using materials that are relatively more economical without the need for expensive molds and tools [2-3], low time and cost [4] and can be done in one time process [5]. Currently, several AM methods have been developed, such as Selective Laser Sintering (SLS) of plastic powders [6], Laminated Object Manufacturing (LOM) of plastic sheets [7], Fused Deposition Modeling filament-based (FDM) [8] and Stereolithography (SLA) based on photopolymer resin [9]. Among several AM techniques, SLA is the 3DP technique with the best printing results in terms of dimensional accuracy [10], surface roughness [3], and low porosity [11].

In the additive manufacturing industry, SLA has undergone significant development, as evidenced by its increasingly widespread application across various fields, including medicine [12]. SLA is an early AM method that uses the solid freeform fabrication (SFF) technique and was introduced by Chuck Hull in 1986 [13]. The SLA three-dimensional (3D) object is based on a spatially controlled solidification process of liquid resin inside a vat resin by photopolymerization. The liquid resin solidification process uses a laser beam or a digital light projector, controlled by a computer, that illuminates the resin surface in a specific pattern to form a hardened layer of a certain thickness until a 3D object is created according to the CAD design [13].

In the additive manufacturing industry, due to the excellent quality of the final product [14] and complex shapes with many under-cut parts, SLA is not only used in the prototype phase but up to the final product that is difficult to achieve through machining processes such as milling [15]. In addition, SLA can be used for rapid prototyping, compared to other traditional manufacturing methods, in small quantities and at a relatively low cost [16]. SLA is often used because it offers several advantages, such as the ability to print complex geometries [17], and SLA prints have better surface roughness than injection molding and FDM [3], [18].

Based on the advantages possessed by SLA, the use of SLA has expanded in several fields, including medicine [12]. In the medical field, several resin materials are commonly used in 3DP SLA machines, including Formlabs resin [19], Anycubic photosensitive resin [20], and Temporis resins [21].

The 3DP SLA machine has several advantages and disadvantages in making 3D specimens. Compared to conventional molding processes such as plastic injection molding, the SLA process has a shorter period [3], SLA printouts also have better dimensional accuracy when compared to FDM [22], SLA is more economical because the process is faster and cheaper than other conventional methods [16], and SLA prints also have better surface roughness compared to injection molding and FDM results [3], [18], [23]. Apart from the advantages that the 3DP SLA machine has, one of the main disadvantages is the low mechanical properties of the printed specimen [2], [24-25], which are affected by the printing parameters used [26].

Many researchers have focused on improving the mechanical properties, surface roughness, and dimensional accuracy of SLA prints using various methods to obtain optimal results. Optimizing printing parameters is one of the simplest and most effective methods [21], [27]. In the tensile test conducted by [19], the results show a significant increase in maximum tensile strength (89% on average) and elastic modulus (89% on average) after the irradiation process. Meanwhile, [20] reported that the hardness of the material increases with increasing irradiation time (hardness and density values are stable after 48 hours of irradiation at a wavelength of 400 nm). In addition, the dimensional accuracy of the samples printed by the SLA from several studies has different assessments, and the best dimensional accuracy is printed with a build orientation of 45° [28-29] and build orientation of 90° [30-31].

In this research, a series of investigations was carried out to determine the effects of LT and NET on the mechanical properties and surface characteristics of PLA materials and those processed by SLA. From the variation of the print parameters, it is expected that the PLA printed specimens with the highest tensile strength and good surface quality.

Table 1
SLA processing parameters used for printing PLA material in this research

Slicing setting	
Layer Thickness (mm)	0.025; 0.05; 0.075
Normal Exposure Time (s)	5; 10; 15
Off Time (s)	0.5
Bottom Exposure Time (s)	40
Bottom Layers	5
Z Lift Distance (mm)	8
Z Lift Speed (mm/s)	2
Z Retract Speed (mm/s)	2
Anti-alias	1
Build orientation (deg)	90
Post process	
Washing time (minute)	5
Curing time (minute)	30

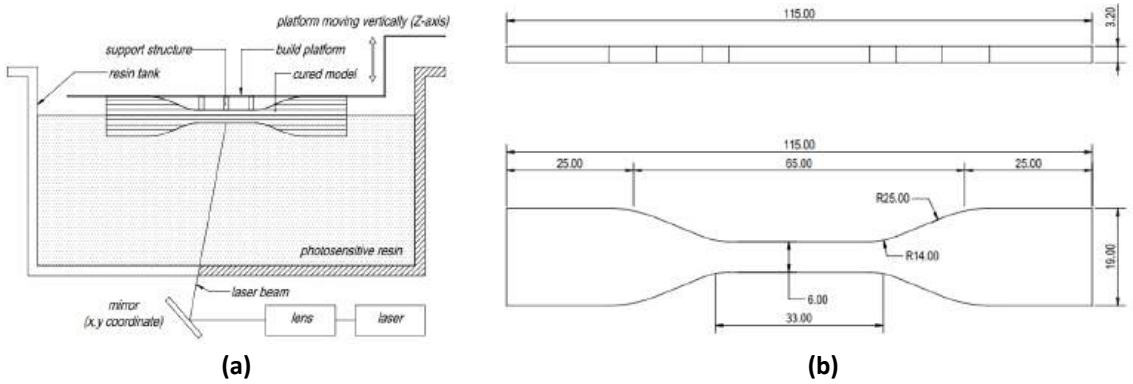

Fig. 1. SLA-processed PLA specimens for tensile test: (a) Specimen print orientation illustration; (b) Dimensions of tensile test specimen

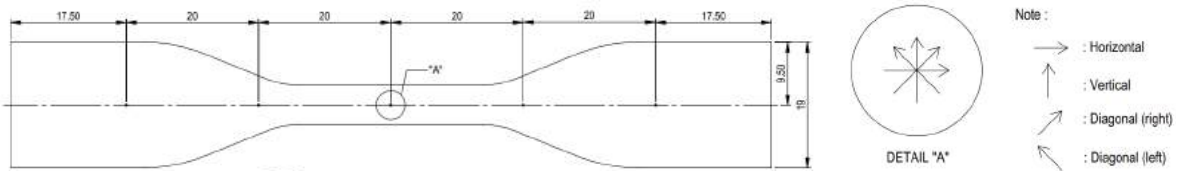

Fig. 2. SLA-processed PLA specimens for surface roughness test (The specimen dimension unit is milimeter)

2. Materials and Methods

In this research, all specimens were made from 3D printing UV Sensitive Basic Clear Anycubic Resin (Shenzen Anycubic Technology Co., Ltd. China), printed using the SLA 3DP Anycubic Photon

Mono X printer (Shenzen Anycubic Technology Co., Ltd. China) and the curing process uses the Anycubic Wash and Cure 2.0 machine (Shenzen Anycubic Technology Co., Ltd. China). The print parameters used for specimen preparation in this study are listed in Tabel 1.

The tensile test was carried out using the dog bone-shaped PLA specimen shown in Figure 1 (b) , which was designed according to the ASTM D638 type IV standard with the specimen position transverse, along the X-axis during the molding process, which orientation is parallel to the tensile loading axis shown in Figure 1 (a). There are nine specimen configuration variations created from Table 1 with the number of specimens for each configuration, namely five specimens. The specimen printing process was carried out at room temperature with a time difference from morning to evening. Then a tensile test was performed using the universal testing machine Zwick Z020 (Zwick/Roell, Germany) at room temperature with a pre-load of 50 N, speed (tensile modulus) 5 mm/min, test speed of 10 mm/min, grip to grip separation at the start position 65 mm, and Gage length (standard travel) 25 mm.

Tensile strength data were obtained, and then post-tensile test specimens with the highest and lowest tensile strength values were analyzed by microstructural testing using an Olympus BX53M microscope (Olympus, Japan) and Scanning Electron Microscope Energy Dispersive X-Ray Phenom Pro X (Phenom, Netherlands) to find out the structure inside the body of the specimen that might affect the tensile strength results obtained previously.

The surface roughness test used the Mitutoyo SJ 210 surface roughness tester stylus (Mitutoyo, Japan) to determine the surface roughness level of the SLA printed specimens affected by LT and NET. The surface roughness test was conducted with four movement directions at five points on one side of the specimen surface, as shown in Figure 2. The surface roughness test was carried out with parameter settings such as ISO 1997 standard, profile R, Gauss filter, λc 2.5, λs 8, and M-speed 0.5.

Test the dimensional accuracy of the SLA printed specimens using a coordinate measuring machine (CMM) Zeiss Calypso SVF NEX (Accretech, Japan) on four measurements, as shown in Figure 3. A one-way ANOVA was finally carried out in Microsoft Excel 2016 (Microsoft, USA) to analyze all the quantitative data obtained from this experiment.

Table 2
PLA material specimen tensile strength

Test	Control (MPa)	LT (mm)	NET 5 second		NET 10 second		NET 15 second	
			$\sigma_{Average}$ (MPa)	STDEV	$\sigma_{Average}$ (MPa)	STDEV	$\sigma_{Average}$ (MPa)	STDEV
Tensile Strength	23.4	0.025	29.9	6.01	33.05	4.58	37.38	7.86
	23.4	0.05	26.8	4.83	37.75	4.35	31.63	6.68
	23.4	0.075	29.62	3.48	30.51	6.58	33.97	4.07
Elongation	14.2	0.025	4.93	1.36	5.23	1.04	7.39	2.37
	14.2	0.05	4.35	1.02	6.96	1.48	5.27	1.83
	14.2	0.075	5.33	1.34	5.0	1.67	4.48	2.03
Young's Modulus	-	0.025	6.16	0.53	6.37	0.38	5.28	0.90
		0.05	6.23	0.40	5.55	0.73	6.20	0.74
		0.075	5.69	0.62	6.43	1.26	6.86	0.96

Notes: Especially Young's modulus using GPa units

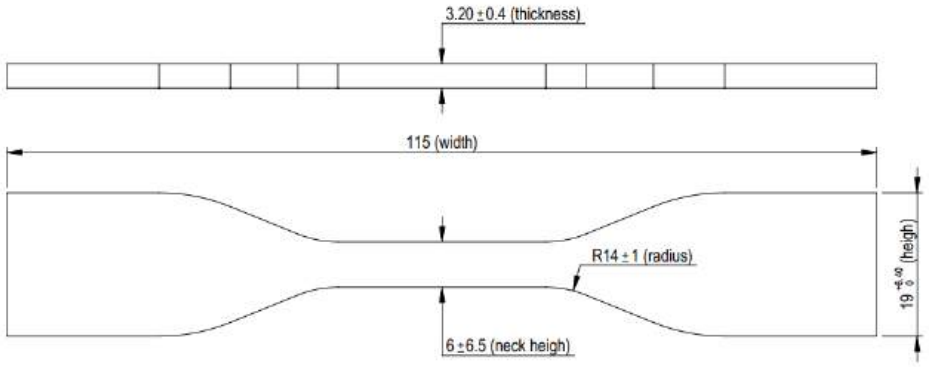

Fig. 3. Measurement dimensions for dimensional accuracy test

3. Results

To avoid environmental changes in the properties of the printed specimens, the authors print the specimens for each test and then store them in an airtight container for the purposes mentioned above. The tests are carried out in parallel. For microstructural observation, the specimens used are post-tensile, especially in the fracture section.

3.1 Tensile Strength of PLA Specimen

The PLA material tensile test results are presented in Table 2 and Figure 4 (a). Control values were taken from the PLA material datasheet used in this study. Table 2 shows the highest average tensile strength of the printed specimens of PLA material of 37.75 MPa at the parameter LT 0.05 mm with NET 10 seconds. In general, the average tensile strength of all parameter variations exceeds the control value. The pattern of values obtained is not in line with the research conducted by [32] and [33] the thinner the LT, the higher the tensile strength value. Tensile strength increases with the addition of layers, where the bond strength between layers is higher than the strength of the layer itself because the cure degree in the interlayer is higher than in the central layer [34]. However, the results showed that the tensile strength of the printed specimen at 0.025 mm LT was lower than that at 0.05 mm LT. This may be due to uncontrolled changes in room temperature during the specimen printing process, which takes about eight hours, such as for 0.025 mm LT specimens (the process passes through time periods when room temperature changes, e.g., morning to evening). In addition, the tensile strength of SLA-printed specimens increases with increasing exposure time. This confirms that increasing exposure time to ultraviolet (UV) light increases the degree of polymerization of free radicals formed when photoinitiators react with UV light [19].

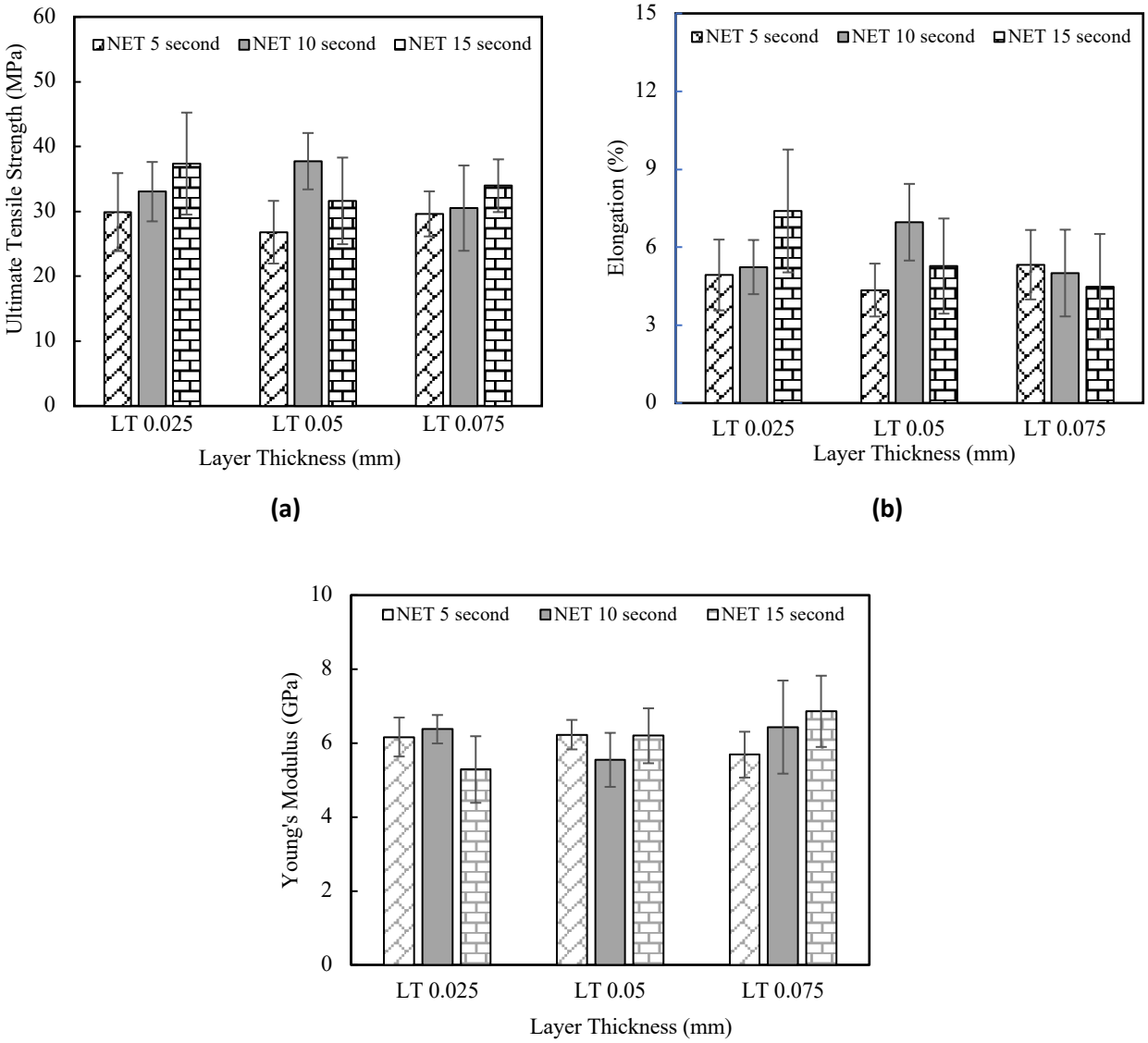

Fig. 4. The effect of LT and NET on the mechanical strength of PLA specimen: (a) Tensile strength; (b) Elongation; (c) Young's Modulus

Figure 4(b) shows that the PLA material specimens with all parameters exhibit elongation values below the control value. In other words, the printed specimens of PLA material are more brittle than the control values in the PLA material datasheet used in this study. This may be due to differences in the temperature of the specimen-printing environment, which can affect the resin's viscosity. The low viscosity of the resin results in small size and molecular weight, leading to increased crosslinked networks in the specimen and brittleness [35].

Figure 4(c) shows that Young's Modulus increases with increasing NET, especially in the 0.075 mm LT specimen. This confirms that increasing UV exposure time (NET) to the resin can reduce the proportion of semi-reacted resin contained in each layer of the SLA printed specimen [36].

3.2 Surface Roughness of PLA Specimen

The overall average surface roughness (Ra) is shown in Table 3. The results of the PLA material surface roughness test shown in Figure 5 (a) and (b) indicate that in a horizontal position, the tendency of the roughness test results is the same, that is, the highest is at NET 5 and the lowest is at NET 15. On the other hand, at LT 0.05 mm, the lowest surface roughness value is observed at NET 10, while the highest is at NET 5, as with the other two LTs.

Table 3
Average Ra of all measurement positions

LT (mm)	Average of Ra (µm)		
	NET 5 second	NET 10 second	NET 15 second
0.025	1.01	0.84	0.93
0.05	1.53	1.45	3.12
0.075	3.55	1.43	2.77

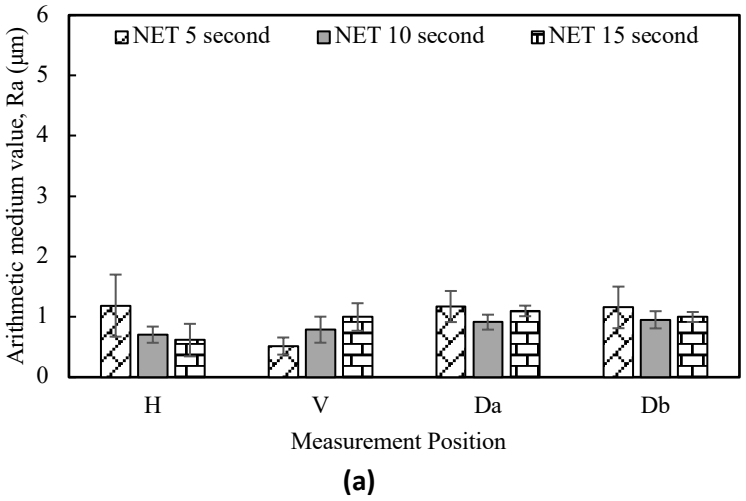

(a)

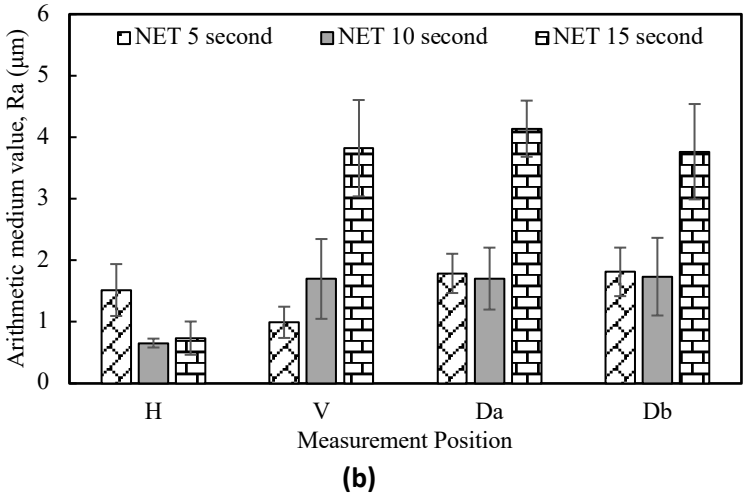

(b)

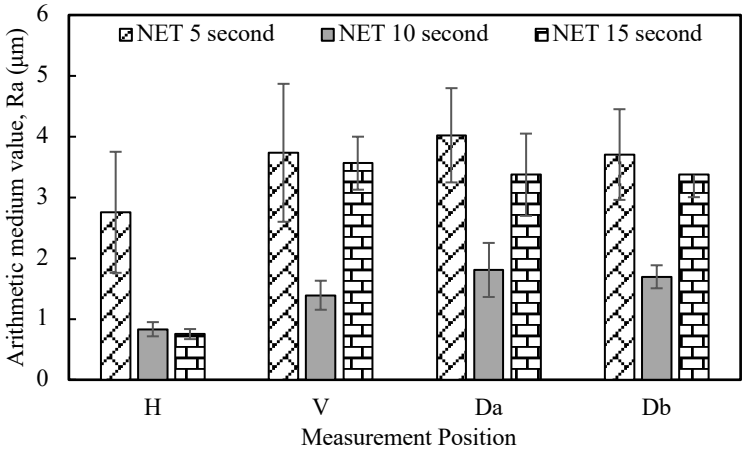

(c)

Fig. 5. PLA material specimen surface roughness: (a) LT 0.025 mm; (b) LT 0.05 mm; (c) LT 0.075 mm

Table 4
The average percentage of dimensional accuracy data errors

LT (mm)	NET (second)		
	5	**10**	**15**
0.025	2.45%	2.27%	3.95%
0.05	2.34%	2.86%	3.81%
0.075	2.14%	2.03%	2.62%

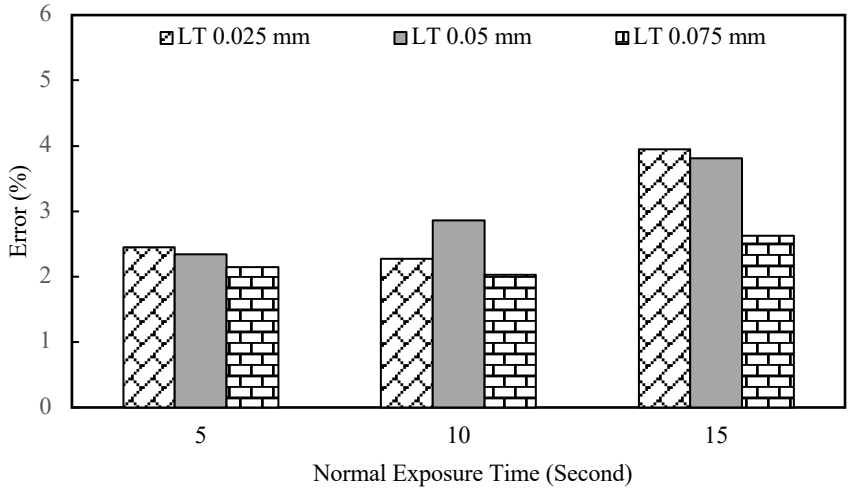

Fig. 6. Average percentage error of dimensional accuracy

In the vertical position, at LT 0.025 and 0.05 mm, the highest surface roughness is at NET 15, and the lowest is at NET 5. On the other hand, at LT 0.075 mm, the highest surface roughness is at NET 5, and the lowest is at NET 10. In the diagonal positions (a) and (b), LT 0.025 and 0.075 mm show the same surface roughness trend, with the highest at NET 5 and the lowest at NET 10 seconds. The same is true for LT 0.05 mm, the lowest roughness value is found at NET 10 seconds. However, at that LT, the highest value is found at NET 15 seconds.

Based on the surface roughness test results, the surface roughness values across all print parameters tend to form random patterns. This is not in accordance with the research that has been conducted by [37] and [38] where the surface roughness level of the SLA printed specimen will increase with the increase in LT (the thicker the LT, the rougher the surface roughness level will be). The randomness of the surface roughness obtained may be due to external factors, such as fluids formed by the up-and-down movement of the build platform, which hit the semireactive layer of the specimen.

3.3 Dimensional Accuracy of PLA Specimen

In this study, dimensional accuracy is defined as the measurement of the outer surface of the SLA-printed specimens (analyzed as the mean absolute deviation), with deviations from this surface measurement considered increasingly inaccurate in both the positive and negative directions. Five-dimensional measurements were taken on the SLA-printed specimens (Figure 3). From the tests conducted, the measurement results were positive, indicating that the specimen had dimensional enlargement relative to the initial design dimensions and vice versa. Table 4 and Figure 6 show the average percentage of errors in the measurements for each dimension mentioned in Figure 3.

The results of the dimensional accuracy test are consistent with the research conducted by [39], which found that the highest dimensional accuracy is obtained at the thickest LT and the shortest NET. In addition, this study is also in accordance with the results of [40] research where the smallest deviation was found at the highest LT. These results do not follow the hypothesis that the smaller the LT, the higher the dimensional accuracy. This confirms that the longer exposure time of UV light to liquid resin causes swelling and the resin's dynamics and degree of polymerization also affect the printed specimens' accuracy [41]. In addition, resins with low viscosity exhibit poor dimensional stability due to their small size and low molecular weight [35].

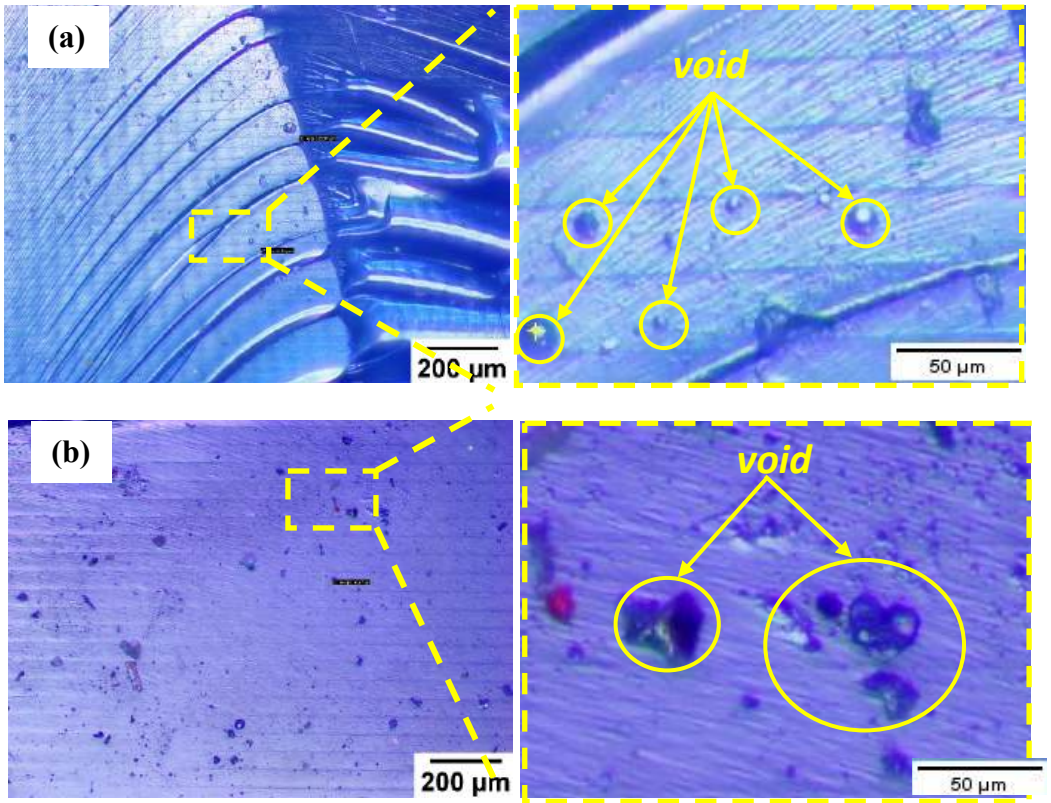

Fig. 7. Voids in the fracture area of the specimen after the tensile test: (a) LT 0.025 mm; (b) LT 0.05 mm

4. Discussion

The influence of print parameters on several tests and the correlation between tests that have been carried out are reviewed with the support of microstructure observation data. The results of microstructure observations are used to support the test results data on the phenomena that occur in the tests that have been carried out. In addition, the validation of the values obtained from each test is compared with the results obtained from several similar previous studies.

The orientation of the specimen prints used in this study is transverse (along the X-axis), as illustrated in Figure 1 (a), where this orientation has the direction of the fibers in the same direction as the direction of the loading force in the tensile test so as to provide the highest tensile strength compared to the orientation of the another prints [42], [43].

The data on the tensile strength of the specimens in the tensile test obtained has a pattern that is not the same as the results of research conducted by [32] and [33] which the thinner the LT, the more the number of layers so that the tensile strength will increase because the more adhesion strength in each layer that withstands the force in the tensile test [44]. For further analysis, microstructure observations in the fracture area of the specimen after the tensile test of PLA material using an Olympus BX53M microscope (Olympus, Japan) complement the reasons for the tensile test results data obtained as shown in Figure 7, where there are voids and several parallel lines which is a connection between layers. The thickness of each layer formed has dimensions close to the LT setting on the 3D printer machine. Voids on the SLA-printed specimens were formed during the photopolymerization process [45]. Voids are more commonly found with larger sizes in specimens with thicker LT, causing a decrease in the mechanical strength of the SLA-printed specimens [32]. Voids can be found in the interlayer bonding and the body of the layer itself [46]. The observed void size is no more than nano size as in the research conducted by [34]. However, the void size is clearly visible in specimens with LT, which are thicker than the LT variation used in this study (LT 0.1 mm), as shown in Figure 8. Interlayer bonding and voids can be observed properly due to the chemical constituents of the PLA resin having a color that light can penetrate with a microscope and has a unique composition. Figure 9 shows that the thicker the LT and the shorter the NET, the more irregular the surface is obtained in the fracture area. This may be due to the increasing thickness of the layer, and the curing rate is lower so that the specimen has a low bond and a rough fracture surface character.

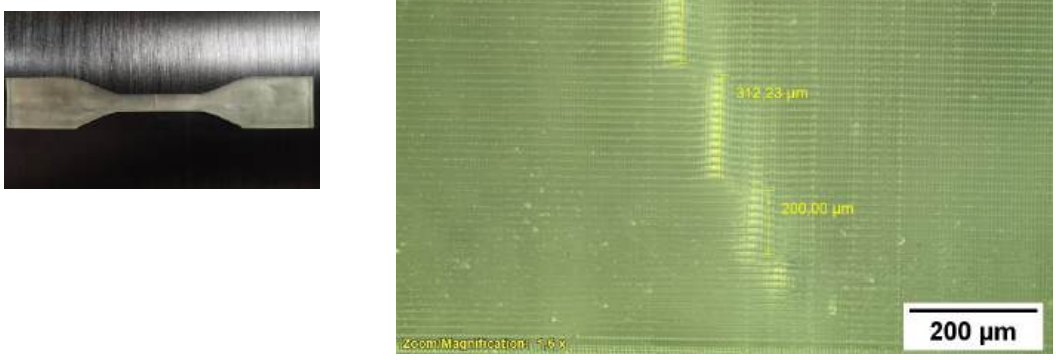

(a)

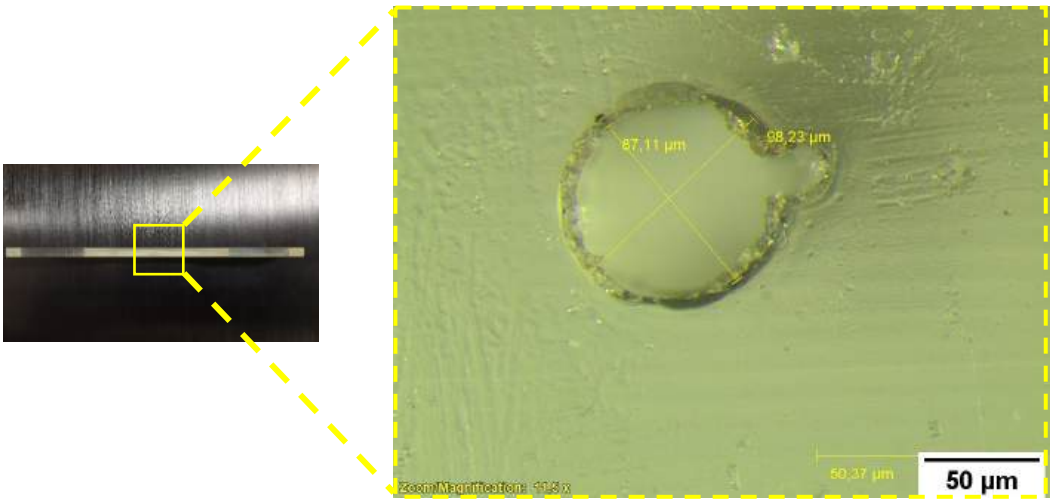

(b)

Fig. 8. Voids on the specimen with LT 0.1 mm (a) void length; (b) void diameter

In addition to mechanical strength, surface roughness and dimensional accuracy of printed specimens are closely related. Both can be affected by process parameters, such as LT resolution, resin material, and polymerization dynamics within the resin during printing [47]. High LT resolution in the Z direction is often assumed to result in high dimensional accuracy and low surface roughness.

In testing the surface roughness, the range of average Ra values obtained is close to the results of research that has been carried out by [37] and [38]. However, the pattern of increasing Ra is different for each LT used, where the level of surface roughness of the printed specimen will increase with the increase in LT. The dimensions of the staircase formed will be larger as the thickness of the LT used is shown in Figure 10. The surface roughness of the SLA printed specimens with the difference in the base material composing the resin will be different, which is due to differences in the chemical elements that make up the resin material [38].

Obtaining one of the high-test results (in this research, namely tensile strength) with such printing parameters does not rule out the possibility of having an impact on other test results, such as dimensional accuracy and surface roughness. Based on data from several tests that have been obtained and the discussion in this sub-chapter, it is known that the print parameters used, such as LT and NET, have a close relationship with the several tests that have been carried out. The use of thinner LT and higher NET will increase tensile strength and minimize surface roughness but can reduce the dimensional accuracy of the printed specimen.

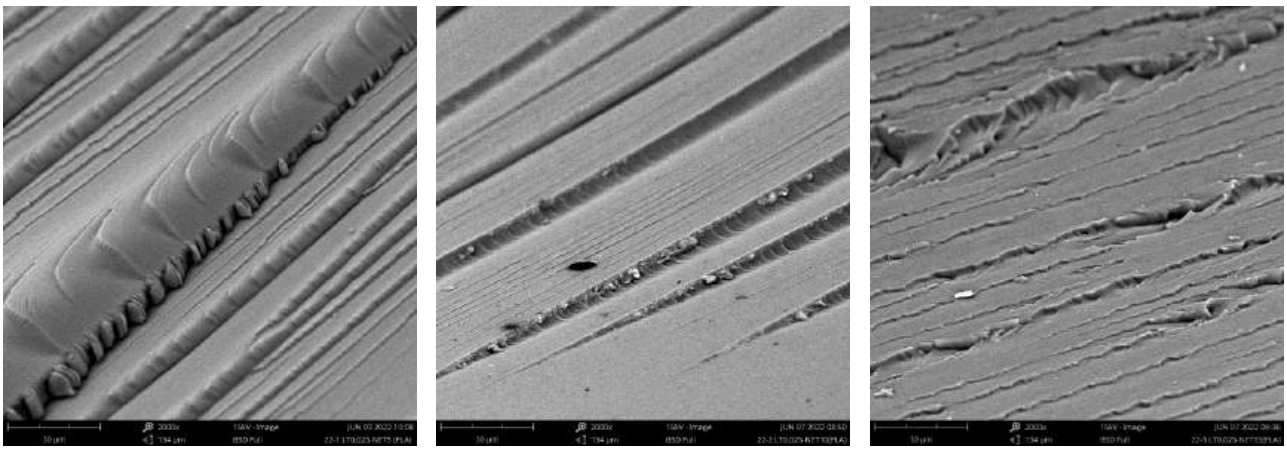

(a) **(b)** **(c)**

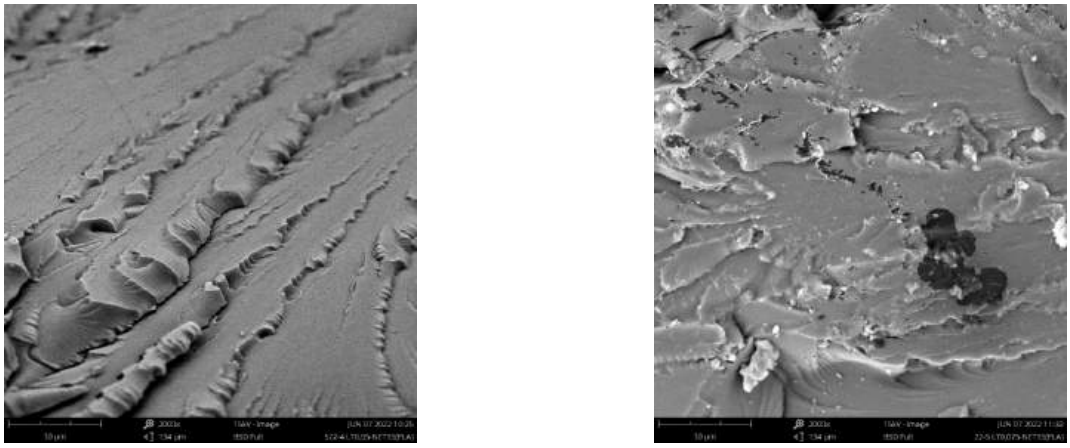

(d) **(e)**

Fig. 9. Fracture surface morphology of PLA parts printed: (a) LT 0.025 mm NET 5 second; (b) LT 0.025 mm NET 10 second; (c) LT 0.025 mm NET 15 second; (d) LT 0.05 mm NET 15 second; (e) LT 0.075 mm NET 15 second

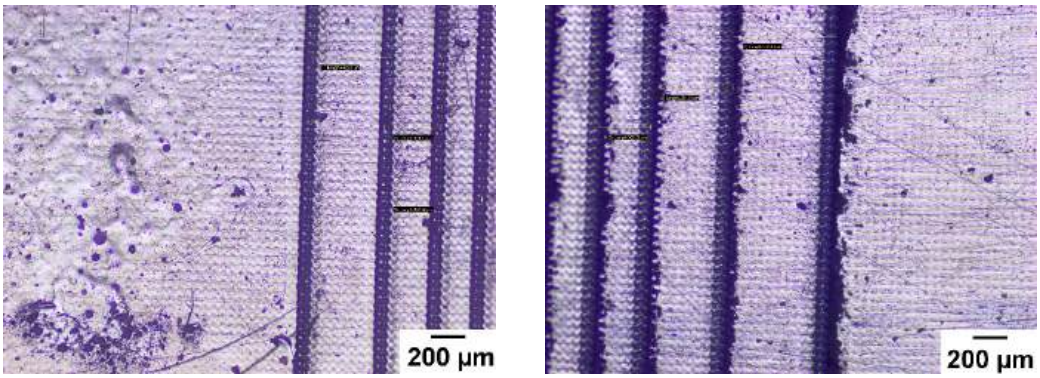

(a) **(b)**

Fig. 10. Staircase effect on the PLA specimen radius area (a) LT 0.025 mm; (b) LT 0.05 mm

Prior to obtaining good specimen printing results with several parameter variations in this research, specimen printing was carried out with other parameter variations, resulting in several failures. This information is used to avoid using the LT parameter and other parameters so that the specimen can be printed properly, such as minimizing voids with dimensions that are large enough so as not to reduce the mechanical strength of the specimen. From several experiments varying process parameters, results indicate that the platform build speed in the Z direction also affects the success of the specimen printing process.

(a) **(b)**

Fig. 11. Printing process failure (a) the neck area is broken; (b) the top layer of the neck area is peeling off

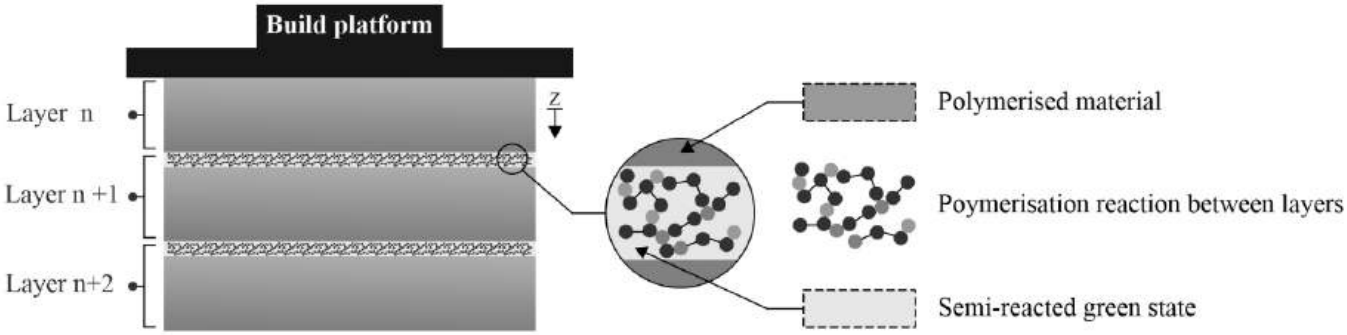

Fig. 12. Illustration of a semireaction layer on SLA printed specimen

The higher the speed of the build platform with a short exposure time, it can cause the specimen to break, as shown in Figure 11 (a), and print failure in the next several layers, as shown in Figure 11 (b). This may be due to the fact that perfect cross linkages have not been achieved in the short exposure time, and the platform build speed is high enough to cause the first layer in the neck area of the specimen to break.

In addition to exposure time and the speed of movement up and down the build platform, LT resolution also affects the success in printing specimens, where the thicker the LT, the lower the level of penetration of UV rays. This causes a decrease in the level of polymerization of the resin, which results in the specimen not being printed perfectly due to the presence of a semi-reaction layer on a layer that has a large enough thickness [48] as illustrated in Figure 12. By selecting a higher resolution, the number of layers needed to print the specimen will increase, as illustrated in Figure 13 (a). Although higher LT resolution allows for more detail and a better surface finish on the printed specimen, it does not necessarily mean that specimens printed with these parameters are more accurate than those with lower LT resolution in terms of deviation from CAD dimensions.

Increasing the LT resolution will increase the potential for errors, artifacts, and failures during the printing process, which results in a decrease in dimensional accuracy and increases the time required in the printing repetition process, where the repetition process will create opportunities for errors to occur [40]. This is confirmed by the data from the dimensional accuracy test results obtained in Table 4, where the highest dimensional accuracy is obtained at the thickest LT and the shortest NET. Thin LT can cause the potential for bleeding of light phenomena, which will occur when the resin material is penetrated and cured too deeply by UV light, as shown in Figure 14 (a), resulting in reduced detail and dimensional accuracy on the Z-axis (shown in the addition the width dimensions of the specimen are in Table 4. Apart from bleeding of light, the thin LT will also cause a scattering effect phenomenon which will occur when the UV rays deviate from the intended straight path resulting in polymerization in an unwanted direction as shown in Figure 14 (b), resulting in reduced detail and dimensional accuracy on the Z and XY axes.

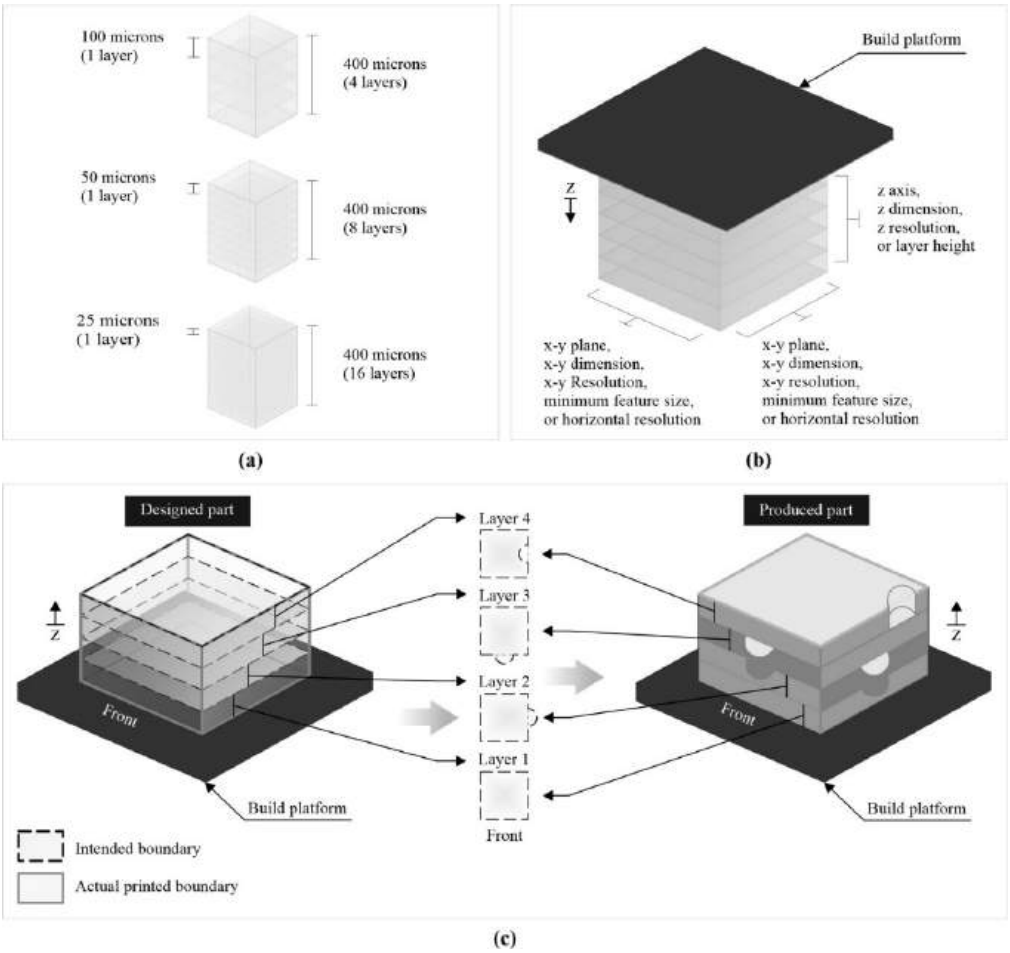

Fig. 13. (a) Visualization of the number of layers per LT, (b) Axis of printing orientation and (c) Effect of XY-axis resolution on the surface of the specimen

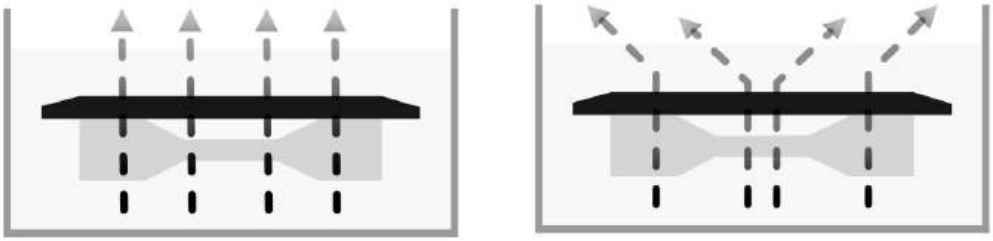

Fig. 14. Type of UV light burst on SLA (a) Bleeding of light; (b) Scattering effect

5. Conclusions

In this research, the influence of print parameters on the mechanical properties and surface characteristics of SLA-treated PLA materials was investigated. Based on the results obtained, it can be concluded that the ranges of LT and NET used in this study, namely LT 0.025, 0.05, and 0.075 mm and NET 5, 10, and 15 seconds, are too narrow to cause changes in mechanical strength (i.e., tensile strength, tensile strain, and elastic modulus) and surface characteristics.

References

[1] Y. Wang, R. Blache, and X. Xu, 'Selection of additive manufacturing processes', *Rapid Prototyp J*, vol. 23, no. 2, pp. 434–447, Mar. 2017, doi: 10.1108/RPJ-09-2015-0123.

[2] B. Arifvianto *et al.*, 'Sliding wear characteristics of FDM-processed polylactic-acid in bovine blood serum', vol. 1, no. 4, pp. 105–112, 2019, doi: https://doi.org/10.15282/jmes.13.4.2019.10.0466 Sliding.
[3] Özdilli Özgür, 'Comparison of the Surface Quality of the Products Manufactured by the Plastic Injection Molding and SLA and FDM Method', *Uluslararası Muhendislik Arastirma ve Gelistirme Dergisi*, no. June, pp. 428–437, Jun. 2021, doi: 10.29137/umagd.762942.
[4] M. Asif *et al.*, 'A new photopolymer extrusion 5-axis 3D printer', *Addit Manuf*, vol. 23, no. June, pp. 355–361, Oct. 2018, doi: 10.1016/j.addma.2018.08.026.
[5] D. G. Bekas, Y. Hou, Y. Liu, and A. Panesar, '3D printing to enable multifunctionality in polymer-based composites: A review', *Compos B Eng*, vol. 179, no. September, p. 107540, Dec. 2019, doi: 10.1016/j.compositesb.2019.107540.
[6] J. Kruth, P. Mercelis, J. Van Vaerenbergh, L. Froyen, and M. Rombouts, 'Binding mechanisms in selective laser sintering and selective laser melting', *Rapid Prototyp J*, vol. 11, no. 1, pp. 26–36, Feb. 2005, doi: 10.1108/13552540510573365.
[7] B. Mueller and D. Kochan, 'Laminated object manufacturing for rapid tooling and patternmaking in foundry industry', *Comput Ind*, vol. 39, no. 1, pp. 47–53, Jun. 1999, doi: 10.1016/S0166-3615(98)00127-4.
[8] M. H. Too *et al.*, 'Investigation of 3D Non-Random Porous Structures by Fused Deposition Modelling', *The International Journal of Advanced Manufacturing Technology*, vol. 19, no. 3, pp. 217–223, Feb. 2002, doi: 10.1007/s001700200016.
[9] M. Gurr and R. Mülhaupt, 'Rapid Prototyping', in *Reference Module in Materials Science and Materials Engineering*, no. March 2015, Elsevier, 2016, pp. 1–27. doi: 10.1016/B978-0-12-803581-8.01477-6.
[10] Y.-G. Jeong, W.-S. Lee, and K.-B. Lee, 'Accuracy evaluation of dental models manufactured by CAD/CAM milling method and 3D printing method', *J Adv Prosthodont*, vol. 10, no. 3, p. 245, 2018, doi: 10.4047/jap.2018.10.3.245.
[11] B. Vieira Magaldi, M. de Oliveira da Costa Maia Pinto, R. Thiré, and A. C. Araujo, 'Comparison of the porosity of scaffolds manufactured by two additive manufacturing technologies: SLA and FDM', in *Procceedings of the 24th ABCM International Congress of Mechanicl Engineering*, ABCM, 2017. doi: 10.26678/ABCM.COBEM2017.COB17-1460.
[12] S. Singh and S. Ramakrishna, 'Biomedical applications of additive manufacturing: Present and future', *Curr Opin Biomed Eng*, vol. 2, pp. 105–115, Jun. 2017, doi: 10.1016/j.cobme.2017.05.006.
[13] H. Gebhardt, *Additive Manufacturing /3D Printing*, vol. 35, no. 3. 2014.
[14] J. Abduo, K. Lyons, and M. Bennamoun, 'Trends in computer-aided manufacturing in prosthodontics: A review of the available streams', *Int J Dent*, vol. 2014, 2014, doi: 10.1155/2014/783948.
[15] Y. Takeda, J. Lau, H. Nouh, and H. Hirayama, 'A 3D printing replication technique for fabricating digital dentures', *Journal of Prosthetic Dentistry*, vol. 124, no. 3, pp. 251–256, 2020, doi: 10.1016/j.prosdent.2019.08.026.
[16] B. Berman, '3-D printing: The new industrial revolution', *Bus Horiz*, vol. 55, no. 2, pp. 155–162, 2012, doi: 10.1016/j.bushor.2011.11.003.
[17] N. Shahrubudin, T. C. Lee, and R. Ramlan, 'An overview on 3D printing technology: Technological, materials, and applications', *Procedia Manuf*, vol. 35, pp. 1286–1296, 2019, doi: 10.1016/j.promfg.2019.06.089.
[18] V. K. Tiwary, A. P., A. S. Deshpande, and N. Rangaswamy, 'Surface enhancement of FDM patterns to be used in rapid investment casting for making medical implants', *Rapid Prototyp J*, vol. 25, no. 5, pp. 904–914, Jun. 2019, doi: 10.1108/RPJ-07-2018-0176.
[19] C. Riccio *et al.*, 'Effects of Curing on Photosensitive Resins in SLA Additive Manufacturing', *Applied Mechanics*, vol. 2, no. 4, pp. 942–955, 2021, doi: 10.3390/applmech2040055.
[20] B. Pszczółkowski and Ł. Dzadz, 'Analysis of the influence of UV light exposure time on hardness and density properties of SLA models', *Technical Sciences*, vol. 23, no. 2020, pp. 175–184, 2020, doi: 10.31648/ts.6119.
[21] N. Alharbi, R. Osman, and D. Wismeijer, 'Effects of build direction on the mechanical properties of 3D-printed complete coverage interim dental restorations', *Journal of Prosthetic Dentistry*, vol. 115, no. 6, pp. 760–767, 2016, doi: 10.1016/j.prosdent.2015.12.002.
[22] J. Nsengimana, J. Van der Walt, E. Pei, and M. Miah, 'Effect of post-processing on the dimensional accuracy of small plastic additive manufactured parts', *Rapid Prototyp J*, vol. 25, no. 1, pp. 1–12, 2019, doi: 10.1108/RPJ-09-2016-0153.
[23] B. Arifvianto, Suyitno, M. Mahardika, P. Dewo, P. T. Iswanto, and U. A. Salim, 'Effect of surface mechanical attrition treatment (SMAT) on microhardness, surface roughness and wettability of AISI 316L', *Mater Chem Phys*, vol. 125, no. 3, pp. 418–426, 2011, doi: 10.1016/j.matchemphys.2010.10.038.
[24] J. Frketic, T. Dickens, and S. Ramakrishnan, 'Automated manufacturing and processing of fiber-reinforced polymer (FRP) composites: An additive review of contemporary and modern techniques for advanced materials manufacturing', *Addit Manuf*, vol. 14, pp. 69–86, Mar. 2017, doi: 10.1016/j.addma.2017.01.003.
[25] J. Pratama *et al.*, 'A review on reinforcement methods for polymeric materials processed using fused filament fabrication (FFF)', *Polymers (Basel)*, vol. 13, no. 22, pp. 1–25, 2021, doi: 10.3390/polym13224022.

[26] R. B. S. Gowda, C. S. Udayagiri, and D. D. Narendra, 'Studies on the Process Parameters of Rapid Prototyping Technique (Stereolithography) for the Betterment of Part Quality', *International Journal of Manufacturing Engineering*, vol. 2014, pp. 1–11, 2014, doi: 10.1155/2014/804705.
[27] N. Alharbi, R. Osman, and D. Wismeijer, 'Factors Influencing the Dimensional Accuracy of 3D-Printed Full-Coverage Dental Restorations Using Stereolithography Technology', *Int J Prosthodont*, vol. 29, no. 5, pp. 503–510, 2016, doi: 10.11607/ijp.4835.
[28] A. Unkovskiy, P. H. B. Bui, C. Schille, J. Geis-Gerstorfer, F. Huettig, and S. Spintzyk, 'Objects build orientation, positioning, and curing influence dimensional accuracy and flexural properties of stereolithographically printed resin', *Dental Materials*, vol. 34, no. 12, pp. e324–e333, 2018, doi: 10.1016/j.dental.2018.09.011.
[29] G.-S. Park, S.-K. Kim, S.-J. Heo, J.-Y. Koak, and D.-G. Seo, 'Effects of Printing Parameters on the Fit of Implant-Supported 3D Printing Resin Prosthetics', *Materials*, vol. 12, no. 16, p. 2533, Aug. 2019, doi: 10.3390/ma12162533.
[30] J. S. Shim, J.-E. Kim, S. H. Jeong, Y. J. Choi, and J. J. Ryu, 'Printing accuracy, mechanical properties, surface characteristics, and microbial adhesion of 3D-printed resins with various printing orientations', *J Prosthet Dent*, vol. 124, no. 4, pp. 468–475, Oct. 2020, doi: 10.1016/j.prosdent.2019.05.034.
[31] A. Unkovskiy, F. Schmidt, F. Beuer, P. Li, S. Spintzyk, and P. K. Fernandez, 'Stereolithography vs. Direct light processing for rapid manufacturing of complete denture bases: An in vitro accuracy analysis', *J Clin Med*, vol. 10, no. 5, pp. 1–14, 2021, doi: 10.3390/jcm10051070.
[32] K. Chockalingam, N. Jawahar, and U. Chandrasekhar, 'Influence of layer thickness on mechanical properties in stereolithography', *Rapid Prototyp J*, vol. 12, no. 2, pp. 106–113, 2006, doi: 10.1108/13552540610652456.
[33] D. Ambrosio, X. Gabrion, P. Malécot, F. Amiot, and S. Thibaud, 'Influence of manufacturing parameters on the mechanical properties of projection stereolithography–manufactured specimens', *International Journal of Advanced Manufacturing Technology*, vol. 106, no. 1–2, pp. 265–277, 2020, doi: 10.1007/s00170-019-04415-5.
[34] M. Kurimoto, Y. Manabe, S. Mitsumoto, and Y. Suzuoki, 'Layer interface effects on dielectric breakdown strength of 3D printed rubber insulator using stereolithography', *Addit Manuf*, vol. 46, no. March, p. 102069, Oct. 2021, doi: 10.1016/j.addma.2021.102069.
[35] M. Pfaffinger, 'Hot Lithography - New Possibilities in Polymer 3D Printing', *Laser Technik Journal*, vol. 15, no. 4, pp. 45–47, Oct. 2018, doi: 10.1002/latj.201800024.
[36] K. W. H. Ahmad, Z. Mohamad, N. Othman, S. H. C. Man, and M. Jusoh, 'The mechanical properties of photopolymer prepared via 3d stereolithography printing: The effect of uv curing time and anisotropy', *Chem Eng Trans*, vol. 78, pp. 565–570, 2020, doi: 10.3303/CET2078095.
[37] C. Arnold, D. Monsees, J. Hey, and R. Schweyen, 'Surface Quality of 3D-Printed Models as a Function of Various Printing Parameters', pp. 1–15, 2019.
[38] K. G. Mostafa, D. S. Nobes, and A. J. Qureshi, 'Investigation of Light-Induced Surface Roughness in Projection Micro-Stereolithography Additive Manufacturing (PμSLA)', *Procedia CIRP*, vol. 92, no. ii, pp. 187–193, 2020, doi: 10.1016/j.procir.2020.05.177.
[39] M. Boca and A. Sover, 'The Printing Parameters Effects on the Dimensional Accuracy of the Parts Made of Photosensitive Resin', vol. 2000287, pp. 1–4, 2021, doi: 10.1002/masy.202000287.
[40] C. S. Favero, J. D. English, B. E. Cozad, J. O. Wirthlin, M. M. Short, and F. K. Kasper, 'Effect of print layer height and printer type on the accuracy of 3-dimensional printed orthodontic models', *American Journal of Orthodontics and Dentofacial Orthopedics*, vol. 152, no. 4, pp. 557–565, 2017, doi: 10.1016/j.ajodo.2017.06.012.
[41] B. Wiedemann and J. Eschl, 'Investigation into the influence of material and process on part distortion', 1995.
[42] R. Quintana, J. W. Choi, K. Puebla, and R. Wicker, 'Effects of build orientation on tensile strength for stereolithography- manufactured ASTM D-638 type i specimens', *International Journal of Advanced Manufacturing Technology*, vol. 46, no. 1–4, pp. 201–215, 2010, doi: 10.1007/s00170-009-2066-z.
[43] K. Puebla, K. Arcaute, R. Quintana, and R. B. Wicker, 'Effects of environmental conditions, aging, and build orientations on the mechanical properties of ASTM type i specimens manufactured via stereolithography', *Rapid Prototyp J*, vol. 18, no. 5, pp. 374–388, 2012, doi: 10.1108/13552541211250373.
[44] P. Kulkarni, A. Marsan, and D. Dutta, 'A review of process planning techniques in layered manufacturing', *Rapid Prototyp J*, vol. 6, no. 1, pp. 18–35, Mar. 2000, doi: 10.1108/13552540010309859.
[45] J. A. Brydson, 'Plastics Materials', in *Plastics Materials*, Boston: Kluwer Academic Publishers, 2005, pp. 153–171. doi: 10.1007/0-306-46908-1_8.
[46] E. A. Papon and A. Haque, 'Tensile properties, void contents, dispersion and fracture behaviour of 3D printed carbon nanofiber reinforced composites', *Journal of Reinforced Plastics and Composites*, vol. 37, no. 6, pp. 381–395, 2018, doi: 10.1177/0731684417750477.
[47] R. P. Chartoff, L. Flach, and P. Weissman, 'Material and Process Parameters that Affect Accuracy in Stereolithography', *Solid Freeform Fabrication Symposium Proceedings*, pp. 245–252, 1993.

[48] P. F. O'Neill, 'Internal void fabrication via mask projection micro-stereolithography : A rapid repeatable microfluidic prototyping technique', no. August, p. 173, 2018.